THE JOURNAL OF BIOLOGICAL CHEMISTRY
Vol. 274, No. 32, Issue of August 6, pp. 22604–22609, 1999

Printed in U.S.A.

Analysis of Receptor Binding by the Channel-forming Toxin Aerolysin Using Surface Plasmon Resonance*

(Received for publication, May 12, 1999, and in revised form, May 28, 1999)

C. Roger MacKenzie‡, Tomoko Hirama‡, and J. Thomas Buckley§¶

From the ‡Institute for Biological Sciences, National Research Council of Canada, Ottawa, Ontario K1A 0R6, Canada and the §Department of Biochemistry and Microbiology, University of Victoria, Victoria, British Columbia V8W 3P6, Canada

Aerolysin is a channel-forming bacterial toxin that binds to glycosylphosphatidylinositol (GPI) anchors on host cell-surface structures. The nature of the receptors and the location of the receptor-binding sites on the toxin molecule were investigated using surface plasmon resonance. Aerolysin bound to the GPI-anchored proteins Thy-1, variant surface glycoprotein, and contactin with similar rate constants and affinities. Enzymatic removal of *N*-linked sugars from Thy-1 did not affect toxin binding, indicating that these sugars are not involved in the high affinity interaction with aerolysin. Aerolysin is a bilobal protein, and both lobes were shown to be required for optimal binding. The large lobe by itself bound Thy-1 with an affinity that was at least 10-fold weaker than that of the whole toxin, whereas the small lobe bound the GPI-anchored protein at least 1000-fold more weakly than the intact toxin. Mutation analyses provided further evidence that both lobes were involved in GPI anchor binding, with certain single amino acid substitutions in either domain leading to reductions in affinity of as much as 100-fold. A variant with single amino acid substitutions in both lobes of the protein was completely unable to bind the receptor. The membrane protein glycophorin, which is heavily glycosylated but not GPI-anchored, bound weakly to immobilized proaerolysin, suggesting that interactions with cell-surface carbohydrate structures other than GPI anchors may partially mediate toxin binding to host cells.

Aerolysin is one of the best characterized of the toxins secreted by pathogenic bacteria (1). The protein is released by *Aeromonas hydrophila* as an inactive 52-kDa precursor called proaerolysin, which is converted to aerolysin by proteolytic removal of a C-terminal peptide (2). Binding of aerolysin to receptors on target cells promotes its oligomerization, and this is followed by membrane insertion and channel formation. Remarkably, all of the proteins that are known to bind aerolysin with high affinity are attached to the cell surface with GPI[1] anchors. These include the erythrocyte aerolysin receptor, brain and T-lymphocyte Thy-1, brain contactin, and VSG of trypanosomes (3–5). We have also shown that cathepsin D, a protein with no affinity for aerolysin, can be converted to an aerolysin-binding protein by addition of a GPI anchor (5), leading to the conclusion that the anchor itself is the major aerolysin binding determinant.

All anchor structures reported to date have a core structure consisting of ethanolamine-HPO_4-6Manα1–2Manα1–6Manα1–4Glc$NH_2\alpha$1–6-*myo*-inositol-1HPO_4 linked to diacylglycerol, alkylacylglycerol, or ceramide. Perhaps not surprisingly, the lipid does not play a role in aerolysin binding: the toxin binds at least as well to GPI-anchored proteins that have been released from cell surfaces by treatment with phosphatidylinositol-specific phospholipase C. The inositol in the core structure can be acylated, and other sugars and/or ethanolamine phosphate can be added to the core mannoses (7). These additions are not always stoichiometric, adding further complexity to anchor structure (8). Not all GPI-anchored proteins can bind aerolysin, at least in some cases because of species differences in modifications to the core structure. Thus, the *Leishmania* protease purified with its naturally occurring anchor attached has no affinity for the toxin, whereas the same protein expressed from the cloned gene in a mammalian cell can bind aerolysin.

Proaerolysin and aerolysin both exist as dimers in solution. Based on the crystal structure of the proaerolysin dimer, each monomer is composed of a small globular lobe containing the first 83 residues joined by a short arm of ~10 amino acids to a large elongated lobe containing the remaining residues (9). Electron microscopic analysis of two-dimensional crystalline arrays of the heptameric aerolysin oligomer indicated that part of the large lobe forms an amphipathic β-barrel that becomes the transmembrane channel upon insertion (9, 10), and a number of residues in this lobe that are involved in the oligomerization process have been identified by chemical modification and site-directed mutagenesis (2). The large lobe may also be involved in receptor binding, based on the observation that the α-toxin of *Clostridium septicum*, which is a homologue of the large lobe of aerolysin, but lacks a region equivalent to the small lobe, can also bind some GPI-anchored proteins (6).[2] However, there is also some evidence that the small lobe is involved in receptor binding. Erythrocytes are far more sensitive to aerolysin than to α-toxin, and fusing the aerolysin small lobe to the clostridial toxin results in a hybrid that is at least as hemolytic as aerolysin (6). The structure of the small lobe also points to a role in carbohydrate binding. We have observed that it is nearly identical to folds in subunits S2 and S3 of pertussis toxin (11), and the common fold, which we have called an aerolysin pertussis toxin (APT) domain, is similar to a fold in C-type lectins and link modules that recognize cell-surface oligosaccharides (11).

Although GPI anchors are clearly the most important determinants of the interaction with aerolysin, there are other prop-

* This work was supported by grants from the Natural Sciences and Engineering Research Council of Canada and the Medical Research Council of Canada (to J. T. B.). The costs of publication of this article were defrayed in part by the payment of page charges. This article must therefore be hereby marked "*advertisement*" in accordance with 18 U.S.C. Section 1734 solely to indicate this fact.

¶ To whom correspondence should be addressed. Tel.: 250-721-7081; Fax: 250-598-6877; E-mail: tbuckley@uvic.ca.

[1] The abbreviations used are: GPI, glycosylphosphatidylinositol; VSG, variant surface glycoprotein; APT, aerolysin pertussis toxin; PAGE, polyacrylamide gel electrophoresis; RU, resonance unit(s).

[2] V. M. Gordon, K. L. Nelson, J. T. Buckley, V. L. Stevens, R. K. Tweten, P. C. Elwood, and S. H. Leppla, manuscript in preparation.

erties of surface proteins that appear to influence toxin binding. For example, we have found that binding to Thy-1 is abolished by protease treatment, indicating that some still uncharacterized feature of the polypeptide chain is required (5). We have also observed that, unlike *C. septicum* α-toxin, aerolysin binds weakly to glycophorin, a heavily glycosylated membrane protein that is not GPI-anchored (6, 12, 13). Fusing the small lobe of aerolysin to the clostridial protein confers glycophorin-binding ability on the resulting hybrid (6). Taken together, the evidence suggests the possibility that aerolysin may contain two carbohydrate recognition sites: one in the large lobe for GPI anchor binding and a second in the small lobe for binding a second carbohydrate determinant, such as is found in glycophorin (6).

In previous studies, the methods used to estimate aerolysin binding have typically been qualitative. Here we describe the use of surface plasmon resonance to obtain quantitative data on aerolysin binding to GPI-anchored proteins and glycophorin. The purified large and small lobes of the toxin as well as a panel of proaerolysin variants were used to investigate the role of each lobe in ligand binding.

EXPERIMENTAL PROCEDURES

GPI-anchored Proteins—Thy-1 was purified from deoxycholate extracts of pig brain using a modification of the procedure of Letarde-Muirhead *et al*. (14). It migrated as a single band upon SDS-PAGE (see Fig. 4). Contactin was isolated from rat brain according to the following procedure. Fresh brain was homogenized (20%, w/v) in ice-cold 0.16 M NaCl, 50 mM Tris, and 1 mM EDTA, pH 8, containing 1 μg/ml pepstatin and 1 mM phenylmethylsulfonyl fluoride. The homogenate (20 ml) was centrifuged at 14,000 × *g* for 10 min, and the pellet was resuspended in the same buffer and washed by recentrifuging. The washed pellet was resuspended to the original volume, and 4 units of phosphatidylinositol-specific phospholipase C (Sigma) were added. Following incubation at 37 °C for 2 h, the mixture was centrifuged, and the supernatant was applied to a column of immobilized lentil lectin. Fractions containing contactin were eluted from the column with 1 M α-methyl-D-mannoside and applied to a column of DEAE-Sepharose CL-6B (Amersham Pharmacia Biotech) equilibrated with 10 mM Tris, pH 8. Contactin was eluted from the column with a linear NaCl gradient. The pooled fractions gave a single band upon SDS-PAGE and silver staining. In addition, a single N-terminal sequence corresponding to the published sequence of contactin was obtained. *Trypanosoma brucei brucei* VSG was a generous gift from Dr. Terry Pearson (University of Victoria). More than 95% of the protein migrated as a single band upon SDS-PAGE.

Deglycosylation of Thy-1—Deglycosylation was performed using the GlycoShift protein de-*N*-glycosylation kit from Oxford GlycoSystems (Oxford, United Kingdom). Thy-1 (4 μg) was incubated with 2 units of enzyme in a total volume of 30 μl for 23 h at 37 °C. Deglycosylation was confirmed by SDS-PAGE.

Proaerolysin Mutants and Truncated Forms of Proaerolysin—The proaerolysin variants listed in Table I were produced by site-directed mutagenesis as described previously (10). In every case, the desired mutation was confirmed by DNA sequencing. Each proaerolysin variant was purified to homogeneity, and its purity was confirmed by SDS-PAGE. All of the variants described in this study could be correctly processed to aerolysin by trypsin, and once processed, they were all capable of forming heptameric oligomers in the same way as native aerolysin. The purification and characterization of the large and small lobes of aerolysin have also been described previously (15).

Biotinylations—Two of the proaerolysin mutants, K171C and E407C, were biotinylated by treating them with 0.2 mM *N*-[6-(biotinamido)hexyl]-3′-(2′-pyridyldithio)propanionamide (Pierce) in 0.15 M NaCl and 20 mM HEPES, pH 7.4, for 90 min at room temperature. Excess reagent was removed by gel filtration.

Surface Plasmon Resonance—Binding kinetics and affinities were determined by surface plasmon resonance using a BIACORE® 1000 biosensor system (Biacore, Inc., Piscataway, NJ) (16). All analyses were performed on research-grade CM5 sensor chips (Biacore, Inc.). Thy-1, VSG, contactin, and streptavidin were immobilized in 10 mM sodium acetate, pH 4.5, at protein concentrations of 5, 10, 10, and 50 μg/ml, respectively, using the amine coupling kit supplied by the manufacturer (Biacore, Inc.). Streptavidin was immobilized at a surface density of 2500 RU. Surface densities of ~1000 RU were used for comparison of wild-type proaerolysin and aerolysin binding to immobilized Thy-1, VSG, and contactin. Surface densities of ~8000 RU were used for comparison of wild-type and mutant proaerolysin binding to native and deglycosylated Thy-1. Proaerolysin variant K171C was immobilized by thiol coupling chemistry, at a surface density of 1750 RU, using the kit provided by the manufacturer (Biacore, Inc.). One RU corresponds to an immobilized protein density of 1 pg/mm^2 (17). Measurements were carried out in 10 mM HEPES, pH 7.4, 150 mM NaCl, 3.4 mM EDTA, and 0.005% P-20 (Biacore, Inc.) at 25 °C and at a flow rate of 10 μl/min. Following analyte binding, surfaces were regenerated with 100 mM HCl and a contact time of 6 s. Sensorgram data were analyzed using BIAevaluation Version 3 software (Biacore, Inc.).

Hemolysis Assay—Titers were determined using washed human erythrocytes according to our published procedure (12).

RESULTS

Mutations in the Small Lobe of Proaerolysin—There are a number of conserved surface residues in the APT domain of the small aerolysin lobe and the two pertussis toxin subunits. These include Trp-45, Ile-47, Tyr-61, and Lys-66 of aerolysin, which cluster on the surface in a way that fully exposes the lysine and the three hydrophobic residues to the solvent (Fig. 1) (11). In addition, Met-57 in aerolysin is fully exposed in a position corresponding to a leucine in S2 and S3. All five of these aerolysin residues seemed likely candidates for receptor interaction, and they were each replaced with another amino acid, producing five variants that were all far less active than native aerolysin in hemolytic titers (Table I). Several other residues in domain 1 were also replaced. These residues are not conserved in the APT fold and hence are less likely to be involved in binding. The activities of these variants were similar to the activity of the wild-type toxin (data not shown).

Mutations in the Large Lobe—For a variety of reasons, we have changed ~50 different residues throughout the large lobe of aerolysin. Many of these changes were found to have no effect on the activity of the protein, whereas others reduced activity by affecting the ability of the toxin to oligomerize or insert (2).[3] Several variants, each with a change at the top of the large lobe, had lower activity than the wild type, and the decrease could not be attributed to changes in oligomerization or insertion. These variants are included in Table I. One of them, C159S, has a free cysteine at 164 and has lost the 159–164 disulfide bridge of the native toxin. Also included in Table I is the variant Y61A/W324A. This variant had no detectable hemolytic activity (Table I), nor was it able to kill T-lymphoma cells, even at concentrations 10^5-fold higher than the wild type (data not shown).

Affinity of Native Aerolysin and Proaerolysin for Different GPI-anchored Proteins—Similar toxin binding profiles were observed for the three GPI-anchored proteins (Thy-1, VSG, and contactin) that were tested as ligands (Fig. 2 and Table II). In addition, there were no significant differences in the kinetics of proaerolysin and aerolysin binding to Thy-1 and contactin. With Thy-1 surfaces, the amount of toxin binding increased after the initial acid regeneration step (Fig. 2), but remained stable throughout subsequent binding and regeneration cycles. A slower dissociation rate constant was responsible for the improved binding on acid-regenerated Thy-1 surfaces (Table II). The rate constants given in Table II were derived by fitting the data to a 1:1 interaction model. In all instances, the fitting was not ideal, but was acceptable if only the early dissociation data were used. The Thy-1 data gave better fitting to this model than the VSG and contactin data and even met the rigorous demands of global fitting (Fig. 3 and Table I). The values obtained for the proaerolysin/Thy-1 interaction by averaging the rate constants derived by local fitting of individual sensor-

[3] C. R. MacKenzie, T. Hirama, and J. T. Buckley, unpublished observations.

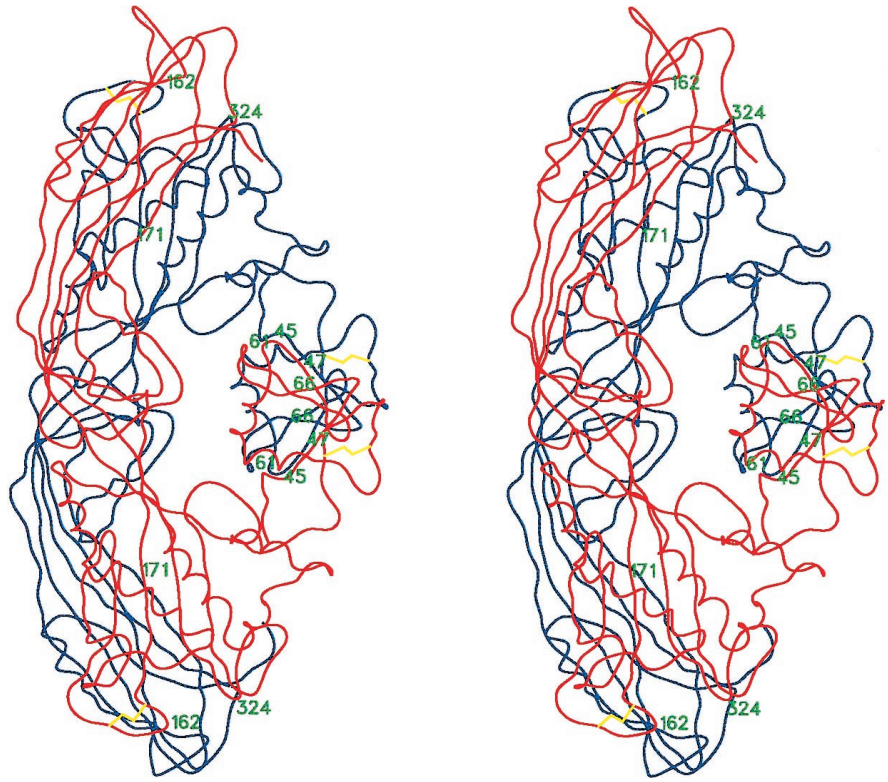

FIG. 1. **Stereo view of the proaerolysin dimer showing key residues involved in GPI anchor binding.** The disulfide bridge between residues 159 and 164 is also shown, as is Lys-171, which may be involved in glycophorin binding (see "Results"). The diagram was prepared using SETOR (20).

TABLE I

Correlation of hemolytic activity with the kinetic and dissociation constants for the binding of wild-type, truncated, and mutant forms of proaerolysin to native and deglycosylated Thy-1

Ligands were directly immobilized on CM5 sensor chips by amine coupling.

Proaerolysin form	Native Thy-1				Deglycosylated Thy-1				
	k_a	k_d	K_o	Relative binding	k_a	k_d	K_o	Relative binding	Hemolytic activity
	$M^{-1}\,s^{-1}$	s^{-1}	M		$M^{-1}s^{-1}$	s^{-1}	M		
Wild type	6.9×10^4 (12%)[a]	7.5×10^{-4} (17%)	1.1×10^{-4} (12%)	100	3.1×10^4 (14%)	7.8×10^{-4} (1%)	2.6×10^{-8} (16%)	100	100[b]
Small lobe			5.0×10^{-5} [c]	0.02			3.7×10^{-5} [c]	0.07	0
Domains 2–4	3.3×10^3 (5%)	2.6×10^{-3} (2%)	8.0×10^{-7} (5%)	1.4	6.3×10^3 (16%)	2.2×10^{-3} (1%)	3.5×10^{-7} (15%)	7.4	0.5
W45A	3.9×10^3 (29%)	1.7×10^{-3} (5%)	4.5×10^{-7} (23%)	2.4	3.9×10^3 (30%)	1.2×10^{-3} (21%)	3.2×10^{-7} (21%)	8.1	2
I47E	1.1×10^3 (34%)	2.6×10^{-3} (24%)	2.9×10^{-6} (57%)	0.4	2.0×10^3 (16%)	8.1×10^{-4} (10%)	4.1×10^{-7} (25%)	63	1
M57A	1.4×10^4 (23%)	1.7×10^{-3} (13%)	1.3×10^{-7} (13%)	8.4	5.9×10^3 (36%)	1.3×10^{-3} (8%)	2.3×10^{-7} (28%)	11	3
Y61A	5.9×10^3 (20%)	1.5×10^{-3} (6%)	2.6×10^{-7} (14%)	4.2	5.2×10^3 (48%)	8.5×10^{-4} (11%)	1.9×10^{-7} (47%)	13	1
K66Q	5.4×10^3 (19%)	2.0×10^{-3} (12%)	3.7×10^{-7} (13%)	3.0	4.3×10^3 (32%)	1.4×10^{-3} (13%)	3.4×10^{-7} (32%)	7.6	1
N154D	6.4×10^4 (18%)	1.1×10^{-3} (2%)	1.7×10^{-8} (18%)	65	5.7×10^4 (39%)	1.2×10^{-3} (11%)	2.3×10^{-8} (37%)	113	25
C159S	8.6×10^4 (39%)	8.3×10^{-3} (3%)	1.1×10^{-7} (35%)	10	3.9×10^4 (14%)	5.7×10^{-3} (5%)	1.5×10^{-7} (16%)	17	6
Y162A	6.0×10^4 (18%)	1.6×10^{-3} (13%)	2.8×10^{-8} (32%)	39	5.0×10^4 (25%)	1.7×10^{-3} (10%)	3.6×10^{-8} (15%)	72	6
K167M	3.9×10^4 (10%)	6.5×10^{-4} (11%)	1.7×10^{-8} (8%)	65	2.6×10^4 (26%)	6.6×10^{-4} (21%)	2.6×10^{-8} (7%)	100	25
K171C	5.6×10^4 (13%)	1.0×10^{-3} (22%)	1.7×10^{-8} (12%)	65	4.2×10^4 (24%)	1.0×10^{-3} (7%)	2.4×10^{-8} (24%)	108	100
W324A	5.8×10^4 (23%)	2.0×10^{-2} (4%)	3.6×10^{-7} (24%)	3.1	3.3×10^4 (44%)	1.5×10^{-2} (5%)	5.6×10^{-7} (47%)	4.6	12.5
H332N	4.0×10^4 (14%)	1.6×10^{-3} (2%)	4.1×10^{-8} (15%)	27	3.4×10^4 (18%)	1.7×10^{-3} (6%)	5.1×10^{-8} (15%)	51	25
E407C	6.1×10^4 (18%)	8.5×10^{-4} (14%)	1.3×10^{-8} (8%)	85	4.2×10^4 (34%)	1.1×10^{-3} (7%)	2.8×10^{-8} (30%)	93	100
Y61A/W324A		NA[d]				NA			0

[a] Values in parentheses are S.D. values based on analyses at five or more concentrations.
[b] As percent of wild-type activity.
[c] Determined by Scatchard analysis.
[d] Not active.

gram data and by global fitting were similar (Table II).

Binding of Proaerolysin Variants and the Small and Large Lobes—Since the data for toxin binding to Thy-1 fit better to a 1:1 interaction model than those collected on VSG and contactin surfaces, Thy-1 surfaces were used for comparison of the ligand binding affinities of wild-type, truncated, and mutant forms of proaerolysin. High density surfaces were required for these comparisons in order to obtain acceptable signals with the lower affinity binders. Local fitting was used in data analysis since the use of high density surfaces gave data that did not always meet the demands of global fitting. Both lobes of proaerolysin were required for full binding activity on Thy-1 surfaces, and binding to Thy-1 was observed with isolated small and large lobes (Table I). The small lobe (domain 1) bound weakly to Thy-1. The data were amenable only to Scatchard analysis because of the rapid kinetics (Fig. 4). Relative to the whole toxin, the K_D for binding of the large lobe (domains 2–4) to Thy-1 (8×10^{-7} M) was >50-fold weaker, and that of the small lobe (5.5×10^{-5} M) was 5000-fold weaker (Table II).

Analysis of mutant binding to immobilized Thy-1 identified several residues in domain 1 and at least one residue in domain 2 that appear most important in ligand binding. The affinities

of the five domain 1 variants (W45A, I47E, M57A, Y61A, and K66Q) were each <5% of the wild-type activity (Table I). In all instances, slower association and faster dissociation rates contributed to the lower affinities. Of the domain 2 variants, only W324A reduced ligand binding affinity to a level that was <5% of the wild-type activity. Among the lower affinity mutants, W324A was unique in that weaker binding was attributable entirely to a faster dissociation rate (Table I). Three other domain 2 mutants (C159S, Y162A, and H332N) showed significantly weaker binding to Thy-1 relative to the wild type (Table I). A double domain 1/domain 2 mutant (Y61A/W324A) was observed to be completely inactive.

There was generally excellent agreement between the affinities determined by surface plasmon resonance and the hemolytic activities of the various forms of proaerolysin (Table I). For example, relative to the wild-type protoxin, the affinity and lytic activity of W45A were reduced ~50- and 75-fold, respectively (Table I). The small and large lobes were both inactive in the titer assay at the concentrations we used. This is consistent with the fact that both lobes are presumably required not only for binding, but for the optimal formation of the insertion-competent oligomer.

Proaerolysin Binding to Deglycosylated Thy-1—Thy-1 was efficiently de-*N*-glycosylated by enzymatic treatment. SDS-PAGE showed a somewhat diffuse band at ~29 kDa for native Thy-1 and a sharp band at ~15 kDa for enzyme-treated Thy-1 (Fig. 5). The profiles for the binding of wild-type whole toxin as well as the truncated and mutant forms to deglycosylated Thy-1 were similar to those observed for native Thy-1 binding (Table I). With the exception of mutant I47E, which bound >10-fold more strongly to the deglycosylated form than to the native form, all truncated and mutant forms of proaerolysin bound to deglycosylated Thy-1 with kinetics and affinities that were very similar to those observed for binding to native Thy-1.

Binding Stoichiometries—Analyte concentrations that were sufficiently high (at least 10 × K_D) to result in near saturation of various surfaces with analyte were used in order to derive information relating to the stoichiometries of toxin/ligand interaction under the experimental conditions employed here. Aerolysin was used at a lower concentration than proaerolysin because it begins to oligomerize at concentrations higher than 200 nM. With Thy-1 surfaces, relatively little of the Thy-1 ligand was available for toxin binding. Toxin/Thy-1 ratios were much lower than 1, based on monovalent binding for both monomeric large lobe and dimeric proaerolysin and aerolysin. In addition, the toxin/Thy-1 ratios were lower for the large lobe relative to proaerolysin and aerolysin and also for deglycosylated Thy-1 relative to native Thy-1 surfaces (Table III).

The binding stoichiometries were also determined using thiol-immobilized K171C, a proaerolysin mutant with wild-

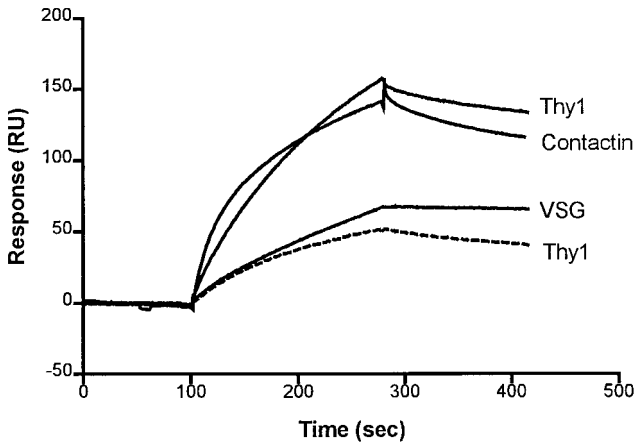

FIG. 2. **Binding of 200 nM proaerolysin to native Thy-1 (*dashed line*) and acid-treated Thy-1, VSG, and contactin surfaces.**

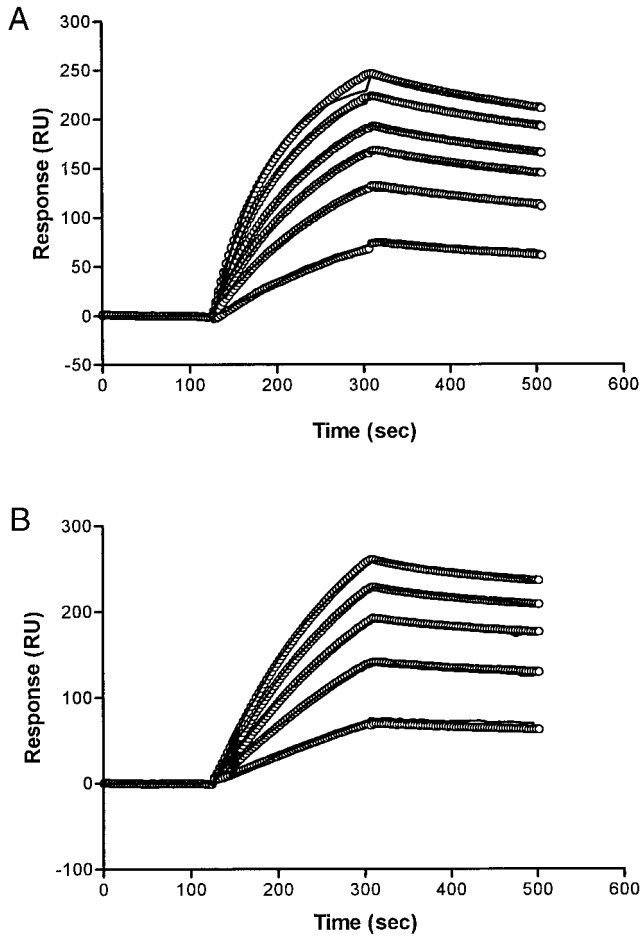

FIG. 3. **Global fitting to a 1:1 interaction of proaerolysin and aerolysin binding to acid-treated Thy-1.** The proaerolysin concentrations were 40, 100, 150, 200, 300, and 400 nM (*A*); the aerolysin concentrations were 40, 80, 120, 160, and 200 nM (*B*). The *open circles* are the data points, and the *solid lines* are the fitted curves.

TABLE II

Kinetics of proaerolysin and aerolysin binding to Thy-1, VSG, and contactin surfaces

Ligands were directly immobilized on CM5 sensor chips by amine coupling.

Immobilized ligand	Curve fitting	Proaerolysin			Aerolysin		
		k_a	k_d	K_D	k_a	k_d	K_D
		$M^{-1}s^{-1}$	s^{-1}	M	$M^{-1}s^{-1}$	s^{-1}	M
Thy-1	Local	3.3×10^4	2.1×10^{-3}	6.6×10^{-8}	ND[a]	ND	ND
Acid-treated Thy-1	Global	3.9×10^4	7.7×10^{-4}	2.0×10^{-8}	2.4×10^4	4.5×10^{-4}	1.9×10^{-8}
Acid-treated Thy-1	Local	5.0×10^4	8.1×10^{-4}	1.8×10^{-8}	ND	ND	ND
Acid-treated VSG	Local	2.0×10^4	6.0×10^{-4}	3.8×10^{-8}	2.8×10^4	3.6×10^{-4}	1.3×10^{-8}
Acid-treated contactin	Local	1.0×10^5	2.3×10^{-3}	2.8×10^{-8}	ND	ND	ND

[a] Not determined.

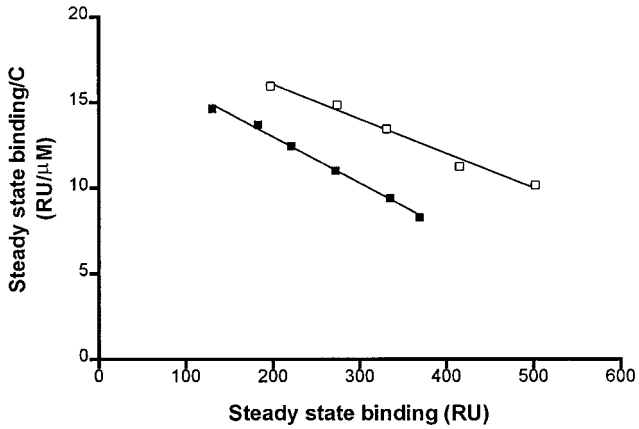

FIG. 4. **Scatchard plots for the determination of proaerolysin affinity for native (*open squares*) and deglycosylated (*closed squares*) Thy-1.**

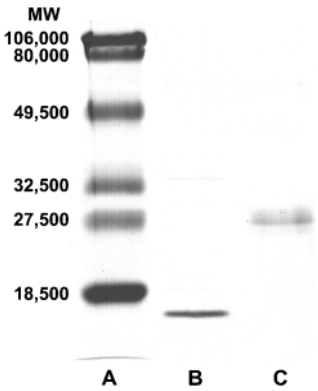

FIG. 5. **Deglycosylation of Thy-1.** Shown are the results from SDS-PAGE of molecular weight markers (*lane A*), deglycosylated Thy-1 (*lane B*), and native Thy-1 (*lane C*).

TABLE III
Interaction stoichiometries of proaerolysin, aerolysin, and domains 2–4 with Thy-1

Molecular masses used in the calculations were 104 kDa for proaerolysin, 95 kDa for aerolysin, 44 kDa for domains 2–4, 30 kDa for Thy-1, and 15 kDa for deglycosylated Thy-1.

Ligand on chip	Analyte	Analyte/ligand
1000 RU native Thy-1	4 μM proaerolysin	0.22
1000 RU native Thy-1	200 nM aerolysin	0.26
1000 RU native Thy-1	8 μM domains 2–4	0.15
1000 RU deglycosylated Thy-1	2 μM proaerolysin	0.06
1750 RU proaerolysin K171C	2 μM native Thy-1	1.8

type activity (Table III). In this orientation, both chains of proaerolysin bound Thy-1. The ratio of bound Thy-1 to immobilized dimer was 1.8 at an analyte concentration of 2 μM. The kinetics of Thy-1 binding to proaerolysin surfaces were similar to those observed in the other orientation (data not shown).

Glycophorin Binding to Proaerolysin—Attempts at immobilizing glycophorin on CM5 sensor chips were unsuccessful, presumably because of the low pI of the protein. To use alternative methods of monitoring the interaction of proaerolysin and glycophorin, two proaerolysin variants with introduced cysteines (E407C and K171C) were used. Both of these variants had similar activities and Thy-1 affinities compared with the wild type (Table I). The K171C variant was readily immobilized on sensor chips by thiol coupling, but attempts at immobilizing E407C in this way were not successful. However, both variants could be captured on streptavidin surfaces following biotinylation. Glycophorin bound to streptavidin-captured E407C (Fig. 6), but not to either streptavidin-captured or thiol-immobilized K171C. The lack of glycophorin binding to K171C was not a result of the immobilization process since Thy-1 bound to both thiol-immobilized K171C and streptavidin-captured K171C (data not shown). Kinetic and affinity constants for binding to E407C were not determined because the binding data could not be fitted to conventional interaction models. This probably reflects varying degrees of multivalent binding arising from the fact that glycophorin is heavily glycosylated and presents multiple copies of carbohydrate structures that can bind to immobilized proaerolysin. However, the low response observed for 20 μM glycophorin binding to 3000 RU of immobilized proaerolysin indicated that this is a very weak interaction. Nevertheless, it is apparently specific since the K171C variant was unable to bind glycophorin, yet was fully active in terms of Thy-1 binding (Table I).

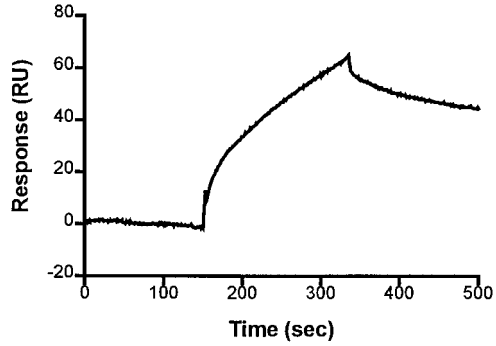

FIG. 6. **Binding of glycophorin to proaerolysin.** Glycophorin (20 μM) was injected over 3000 RU of biotinylated E407C captured on a streptavidin surface.

DISCUSSION

The results of the present quantitative analysis of aerolysin binding using surface plasmon resonance allow us to draw several important conclusions about the nature of the interaction between the toxin and its receptors. Perhaps most important, the results show that both the small lobe of the toxin and a region at the top of the large lobe are involved in binding to GPI anchors. This conclusion is consistent with the circumstantial evidence we had before we began this study. Thus, we had observed that the small lobe of the toxin has a fold that we have called the APT domain (Fig. 1), which is similar to the carbohydrate recognition domain of the C-type lectins and other proteins. Changing any of the five conserved surface-exposed residues in the aerolysin APT domain had a profound effect on binding to Thy-1 (Table I). This was due to a decrease in the interaction of the small lobe with the glycosyl portion of the anchor, rather than with the *N*-linked sugars of Thy-1, since proaerolysin and aerolysin bound at least as well to de-*N*-glycosylated Thy-1 as to the native glycoprotein. Changing residues in the small lobe that are not conserved in the APT fold had little or no effect on binding (data not shown).

The observation that *C. septicum* α-toxin also binds GPI-anchored proteins, despite the fact that it lacks a region homologous to the small lobe of aerolysin, suggested that the large lobe is also capable of binding the anchor, and this, too, was confirmed in this study. In fact, the results in Table I show that the large lobe by itself bound better to Thy-1 than the purified small lobe. This interaction appears to involve the top of the large lobe, in the region we have called domain 2. Removing the disulfide bridge by replacing Cys-159 with serine or changing a number of nearby residues, most notably Tyr-162 and Trp-324 (Fig. 1), all reduced aerolysin binding to Thy-1. It

should be noted that we have changed >40 other residues throughout the large lobe with no apparent effects on receptor binding, more evidence that it is the top of the large lobe that contributes to binding.

In common with other carbohydrate-binding proteins, the GPI-binding site of aerolysin contains numerous aromatic residues. In carbohydrate-binding proteins, the side chains of aromatic amino acids frequently stack against the hydrophobic faces of sugar rings (18). Clearly, two proaerolysin residues (Tyr-62 in the small lobe and Trp-324 in the large lobe) are crucial for binding since the double mutant Y61A/W324A was inactive. These residues are close to each other in the aerolysin dimer, raising the possibility that initial toxin binding to individual GPI anchors may involve both monomers. The mutation studies indicated that a third aromatic residue, Trp-34, was also a component of the ligand-binding site. The significant clustering of aromatic residues on the surface of domain 2 (9) suggests a probable role for additional domain 2 residues in binding. The origin of the dramatic effect of the I47E mutation on binding (Table I) is not clear, but may relate more to the introduction of a negative charge than to alteration of the ligand-binding site. Significantly, the effect was much more pronounced with native Thy-1 than with deglycosylated Thy-1. With native Thy-1, this mutation reduced the affinity to less than that of the large lobe. Also, the effect of the C159S mutation (Table I) may not reflect direct alteration of a ligand contact residue, but may be due to the loss of the 159–164 disulfide bridge.

With a K_D in the vicinity of 20 nM, the interaction of aerolysin with the Thy-1 anchor is very high affinity for protein-carbohydrate binding. The K_D values for these kinds of interactions are more typically in the micromolar range (18). The core GPI structure has two phosphate groups (7) that could interact ionically with the toxin and contribute to the unusually high affinity. The observation that the K66Q mutation reduced proaerolysin affinity for Thy-1 (Table I) supports this possibility. It has been observed that antibodies specific for oligosaccharides containing 3-deoxy-D-manno-2-octulosonic acid also have affinities in the nanomolar range, and this has been attributed to the presence of charged groups on the antigens.[4]

The dissociation kinetics indicated monovalent binding of proaerolysin and aerolysin dimers to immobilized Thy-1. The avidity effect associated with bivalent binding would result in dramatically slower dissociation rate constants, and the k_d for the interaction of monomeric large lobe with native Thy-1 was only 3-fold faster than that of the dimeric protoxin (Table I). Also, the binding stoichiometries were consistent with monovalent binding of the bivalent toxin molecules. The reasons for the low toxin/Thy-1 ratios on Thy-1 surfaces under near saturation conditions are not clear, but are presumably related to poor accessibility of the GPI anchor to the toxin. It is possible that Thy-1 molecules are immobilized in an orientation that obstructs binding. Alternatively, accessibility may be affected by Thy-1 aggregation, through the lipid tails, on the sensor chip surfaces. Interestingly, Thy-1 accessibility was less restricted with native Thy-1 relative to deglycosylated Thy-1 and for intact forms of the toxin relative to the large lobe.

Our results also confirm that aerolysin can bind to erythrocyte glycophorin, although the interaction is considerably weaker than the interaction with any of the GPI-anchored proteins. The fact that the K171C variant was unable to bind glycophorin, although it could bind Thy-1, indicates that the binding site for sugars of the erythrocyte protein is at least partly different from the binding site for the GPI anchor. It is possible that there is an ionic interaction between the lysine side chain at position 171 of the toxin and the acidic sugars displayed on glycophorin. Residue 171 is located in domain 2, with its side chain pointing away from the surface of proaerolysin opposite the interface between the two chains (Fig. 1). It is in relatively close proximity to domain 1 of the other chain of the dimer. Domain 1 has been previously implicated in glycophorin binding (10). Interestingly, the region of domain 1 of the adjoining chain that is closest to Lys-171 has two lysines at positions 66 and 67 (Fig. 1). In the assays performed here, any interaction between proaerolysin and the *N*- and *O*-linked sugars on Thy-1 would be completely masked by the strong binding to the GPI anchor. However, it is possible that the initial interaction of the toxin with host cells involves carbohydrate structures more distant from the membrane surface than GPI anchors, such as the *N*-linked sugars of Thy-1 and the sugars of glycophorin. Such a mechanism for binding might explain how aerolysin penetrates the cell's glycocalyx, and it would be analogous to that observed in the inflammatory response wherein the low affinity selectin/oligosaccharide interaction is followed by a stronger interaction between cell adhesion molecules and integrins (19). In addition, it would explain the dramatic increase in hemolytic activity observed when the small lobe of aerolysin, itself inactive, is fused to the weakly hemolytic *C. septicum* α-toxin.

Acknowledgments—We thank Rebecca To and Dr. S. V. Evans for generating the stereo diagram of proaerolysin. The technical assistance of Tracy Lawrence, Kim Nelson, and Miranda Tradewell is also gratefully acknowledged.

[4] S. Müller-Loennies, C. R. MacKenzie, S. I. Patenaude, S. V. Evans, P. Kosma, H. Brade, L. Brade, and S. Narang, manuscript in preparation.

REFERENCES

1. Lacy, D. B., and Stevens, R. C. (1998) *Curr. Opin. Struct. Biol.* **8,** 778–784
2. Parker, M. W., van der Goot, F. G., and Buckley, J. T. (1996) *Mol. Microbiol.* **19,** 205–212
3. Cowell, S., Aschauer, W., Gruber, H. J., Nelson, K. L., and Buckley, J. T. (1997) *Mol. Microbiol.* **25,** 343–350
4. Nelson, K., Raja, S. M., and Buckley, J. T. (1997) *J. Biol. Chem.* **272,** 12170–12174
5. Diep, D. B., Nelson, K. L., Raja, S. M., Pleshak, E. N., and Buckley, J. T. (1998) *J. Biol. Chem.* **273,** 2355–2360
6. Diep, D. B., Nelson, K. L., Lawrence, T. S., Sellman, B. R., Tweten, R. K., and Buckley, J. T. (1999) *Mol. Microbiol.* **31,** 785–794
7. Schneider, P., and Ferguson, M. A. J. (1995) *Methods Enzymol.* **250,** 614–630
8. Mehlert, A., Richardson, J. M., and Ferguson, M. A. J. (1998) *J. Mol. Biol.* **277,** 379–392
9. Parker, M. W., Buckley, J. T., Postma, J. P. M., Tucker, A. D., Leonard, K., Pattus, F., and Tsernoglou, D. (1994) *Nature* **367,** 292–295
10. Buckley, J. T., Wilmsen, H. U., Lesieur, C., Schulze, A., Pattus, F., Parker, M. W., and van der Groot, F. G. (1995) *Biochemistry* **34,** 16450–16455
11. Rossjohn, J., Buckley, J. T., Hazes, B, Murzin, A. G., Read, R., and Parker, M. W. (1997) *EMBO J.* **16,** 3426–3434
12. Garland, W. J., and Buckley, J. T (1988) *Infect. Immun.* **56,** 1249–1253
13. Howard, S. P., and Buckley, J. T. (1982) *Biochemistry* **21,** 1662–1667
14. Letarde-Muirhead, M., Barclay, A. N., and Williams A. F. (1975) *Biochem. J.* **151,** 685–697
15. Diep, D. B., Lawrence, T. S., Ausio, J., Howard, S. P., and Buckley, J. T. (1998) *Mol. Microbiol.* **30,** 341–352
16. Jönsson, U., Fägerstam, L., Ivarsson, B., Johnsson, B., Karlsson, R., Lundh, K., Löfås, S., Persson, B., Roos, H., Rönnberg, I., Sjölander, S., Stenberg, E., Ståhlberg, R., Urbaniczky, C., Östlin, H., and Malmqvist, M. (1991) *BioTechniques* **11,** 620–627
17. Stenberg, E., Persson, B., Roos, H., and Urbaniczky, C. (1991) *J. Colloid Interface Sci.* **143,** 513–526
18. Evans, S. V., and MacKenzie, C. R. (1999) *J. Mol Recognit.*, in press
19. Simanek, E. E., McGarvey, G. J., Jablonowski, J. A., and Wong, C.-H. (1998) *Chem. Rev.* **98,** 833–862
20. Evans, S. V. (1993) *J. Mol. Graphics* **11,** 134–138

Analysis of Receptor Binding by the Channel-forming Toxin Aerolysin Using Surface Plasmon Resonance

C. Roger MacKenzie, Tomoko Hirama and J. Thomas Buckley

J. Biol. Chem. 1999, 274:22604-22609.
doi: 10.1074/jbc.274.32.22604